Proc. Lunar Sci. Conf. 6th (1975), p. 79–99.
Printed in the United States of America

Geology, petrology, and crystallization of Apollo 15 quartz-normative basalts

G. E. LOFGREN

NASA Johnson Space Center, Houston, Texas 77058

C. H. DONALDSON*

The Lunar Science Institute, Houston, Texas 77058

T. M. USSELMAN

NASA Johnson Space Center, Houston, Texas 77058

Abstract—The quartz-normative (QN) basalts collected at the Apollo 15 site have a unique and consistent bulk chemistry, but display a systematic variation in phenocryst morphology and matrix texture. Experimental crystallization studies show that the textural variation is primarily the result of differences in cooling rate. Quantitative cooling rates are placed on the QN basalts by comparison of their phenocryst and matrix crystal morphologies with those in the experimentally crystallized QN basalts. Cooling rates at which phenocrysts grew (< 1 to 20°C/hr) are often slightly less than the cooling rates at which matrix crystals grew (< 1 to > 30°C/hr). Rather than indicating a two-stage origin for the porphyritic texture, this cooling rate discrepancy is explained, in part, by calculations on the cooling of a lava flow which indicate that the cooling rate increases with decreasing temperature in the central part of a lava flow, and, in part, by the experiments in which changes in nucleation density and oxygen fugacity during crystallization modify the texture developed at linear cooling rates. A review of the geologic and chemical data combined with the experimental results on the QN basalts indicate that they are most likely part of a single 2–3 m-thick lava flow that reached the lunar surface essentially free of crystals. The magma is probably the low-pressure fractionation product of an olivine basalt that is not related to the olivine-normative basalt that overlies it at the Apollo 15 site.

INTRODUCTION

THE QUARTZ-NORMATIVE (QN) BASALTS collected at the Apollo 15 landing site display a variety of textures (LSPET, 1972; Brown *et al.*, 1972; Dowty *et al.*, 1974) and a very uniform major-element chemistry (Rhodes and Hubbard, 1973; Chappel and Green, 1973). Chappel and Green (1973) suggest that the textural variants are samples from various positions in a rock unit (?lava flow). The QN basalts are porphyritic with pigeonite phenocrysts, usually rimmed by augite, set in a matrix that varies from cryptocrystalline to spherulitic to radiate to subophitic. Olivine is present as sparse phenocrysts usually in the more rapidly cooled rocks.

We demonstrated in a previous paper (Lofgren *et al.*, 1974) that the rock textures and crystal morphologies of the QN basalts could be duplicated

*Present address: Department of Geology, University of Manchester, Manchester M13 9PL, England.

experimentally. In this paper we place ranges of cooling rate on the QN basalts by direct comparison of phenocryst morphologies and rock textures with samples produced experimentally at known linear cooling rates. This comparison shows that although crystallization at linear cooling rates produces porphyritic textures similar to those in the natural rocks, other variables such as nucleation and oxygen fugacity appear to play a role in producing slight variations. From the cooling rate data, a minimum estimate can be made of thickness of the lava flow.

This experimental crystallization study indicates that the QN basalt samples are representative of a rapidly cooled, wholly molten lava. Weigand and Hollister (1973) and Dowty *et al.* (1974) have come to the same conclusion based on petrographic, crystallographic, and chemical studies. Bence and Papike (1972) present two models, one based on rapid crystallization of a liquid on the surface and the other based suppression of plagioclase and early clinopyroxene precipitation at depth. Humphries *et al.* (1972) maintain that the phenocrysts were present upon eruption. Thus it is appropriate to review this evidence, in addition to the largely ignored geologic evidence (Swann *et al.*, 1972; Howard *et al.*, 1972), and establish the state of knowledge of the quartz-normative basalts.

COOLING AND CRYSTALLIZATION HISTORY

Relative cooling rates

The pyroxene phenocryst morphologies and matrix textures of the QN basalts greater than 40 g have been ranked in order of relative cooling rate (Table 1; Figs. 1 and 2), based on the experimental determination of crystal morphology versus cooling rate (Lofgren *et al.*, 1974). The phenocrysts and groundmass crystals are ranked separately and show little variance in their relative order.

The pyroxene phenocrysts and matrix textures can be placed in four groups. The phenocrysts range from highly skeletal to anhedral and subsequant and the matrix textures from cryptocrystalline to subophitic (Table 2). The most distinct break in texture and crystal size occurs between the vitrophyric spherulitic and the porphyritic radiate basalts principally in the size of the phenocrysts. Groups I and II of LSPET (1972) and Brown *et al.* (1972) are considered textural variants of the QN basalt lava and are related to the locality at which they were collected (see geologic setting).

This classification and ranking by cooling rate is in general accord with similar attempts to determine relative cooling rates based on petrography. Weigand and Hollister (1973) suggest that 15597 is the most rapidly cooled QN basalt based on extreme Fe, Ti, and Al enrichment in the augitic rims of the phenocrysts relative to other vitrophyres. They also consider the phenocrysts to be less skeletal than 15485 and 15486. This corresponds to the experimental data indicating that 15597 has the most rapidly cooled matrix and less rapidly cooled phenocrysts. Brown and Wechsler (1973) suggest a reheating episode for this rock, possibly by latent heat of crystallization or subsequent reheating and devitrification, to sharpen the "b" reflections in the pyroxene phenocrysts.

Table 1. Apollo 15 quartz-normative rocks of greater than 40 g are ranked according to cooling rate on the basis of the phenocryst shapes and matrix textures. Cooling rates are estimated from comparison with linear cooling rate runs (Lofgren *et al.*, 1974). Numbers in parentheses are rake samples for which we have not seen thin sections; these are tentatively ranked on the basis of the illustrations of Dowty *et al.* (1974).

Pyroxene phenocrysts		Matrix	
485	↑	597	↑
486		(125)	>30°C/hr
597	5–20°C/hr	485	f_{O_2} change?
499	↓	486	↓
(125)	↑	595	↑
595		499	
596	2–5°C/hr	(666)	10–30°C/hr
(666)		596	↓
(682)	↓	(682)	↑
(118)	↑	476	
476		495	1–5°C/hr
495		(118)	
475		(684)	↓
(684)		475	↑
058	<1°C/hr	058	
075		076	
076		075	<1°C/hr
(116)		(116)	
065		065	
085	↓	085	↓

Papike *et al.* (1972) show that the subsolidus cooling rate of 15499 exceeds that of 15058 based on the magnitude of the differences in the β angle between the core pigeonite and the mantling augite of the phenocrysts. Using the same criterion, Takeda *et al.* (1975) show that 15495 cooled faster than 15058. Dowty *et al.* (1974) use chemical, petrographic, and crystallographic data to place relative cooling rates on six QN basalt rake samples (see Table 1; rock numbers in parenthesis). Comparison of photomicrographs of these samples with the large rock samples allows their location in Table 1. The sequence determined by Dowty *et al.* (1974) is unaltered.

Quantitative cooling rates

Cooling rate ranges are placed on the QN basalts (Table 1) by direct comparison of crystal morphology between the natural samples and those grown experimentally at known cooling rates from a melt of equivalent composition (Lofgren *et al.*, 1974). The changes of crystal morphology with cooling rate are only sensitive enough to give ranges of possible cooling rates for a given

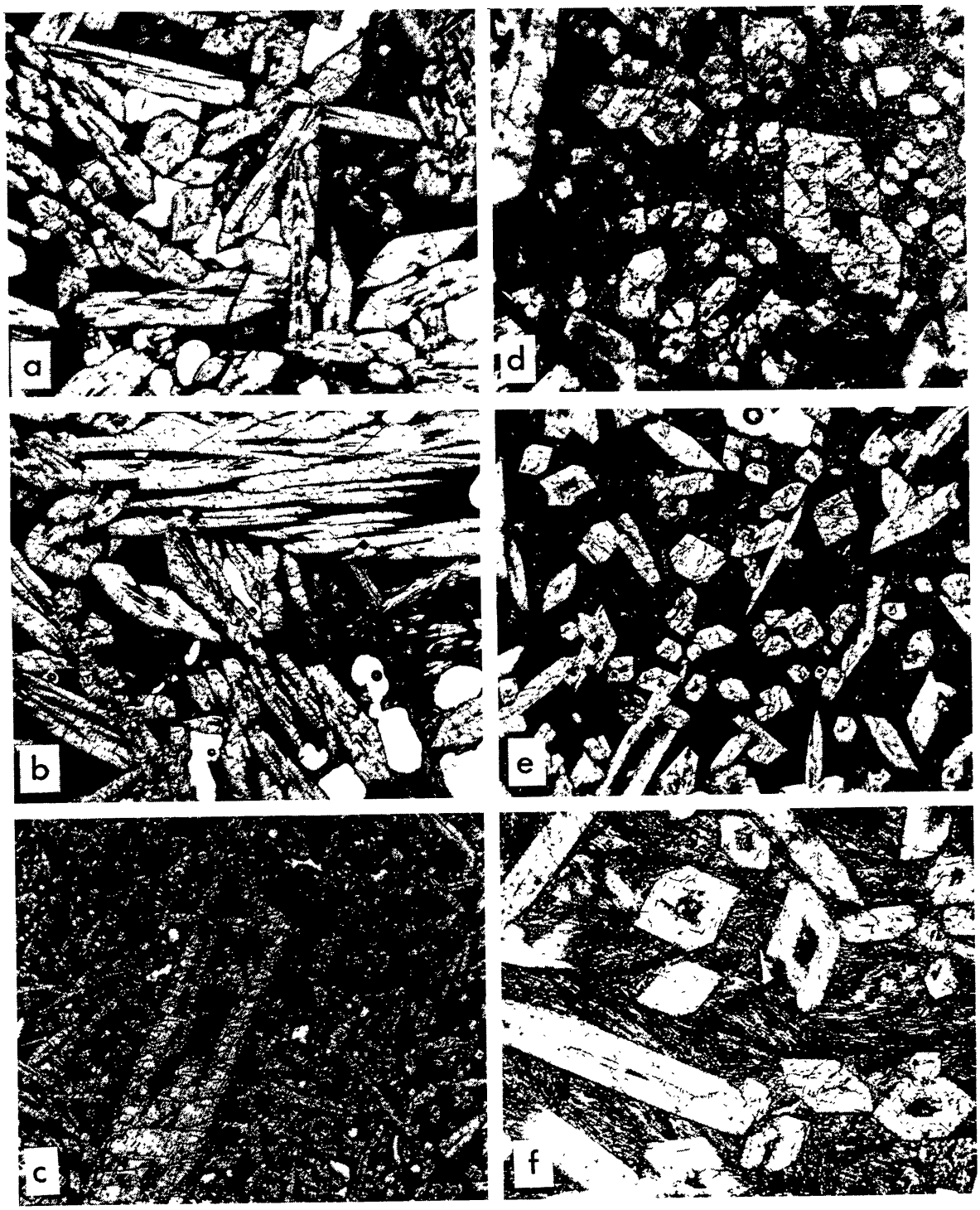

Fig. 1. Quartz-normative basalts ranked in order of decreasing cooling rate at which the phenocrysts grew (Table 1). Vitrophyric basalts are shown in a–c and porphyritic spherulitic basalts in d–f (Table 2). Each photomicrograph is 4.5 mm wide: (a) 15485,6; (b) 15486,21; (c) 15597,17; (d) 15499,6; (e) 15595,37; and (f) 15596,16.

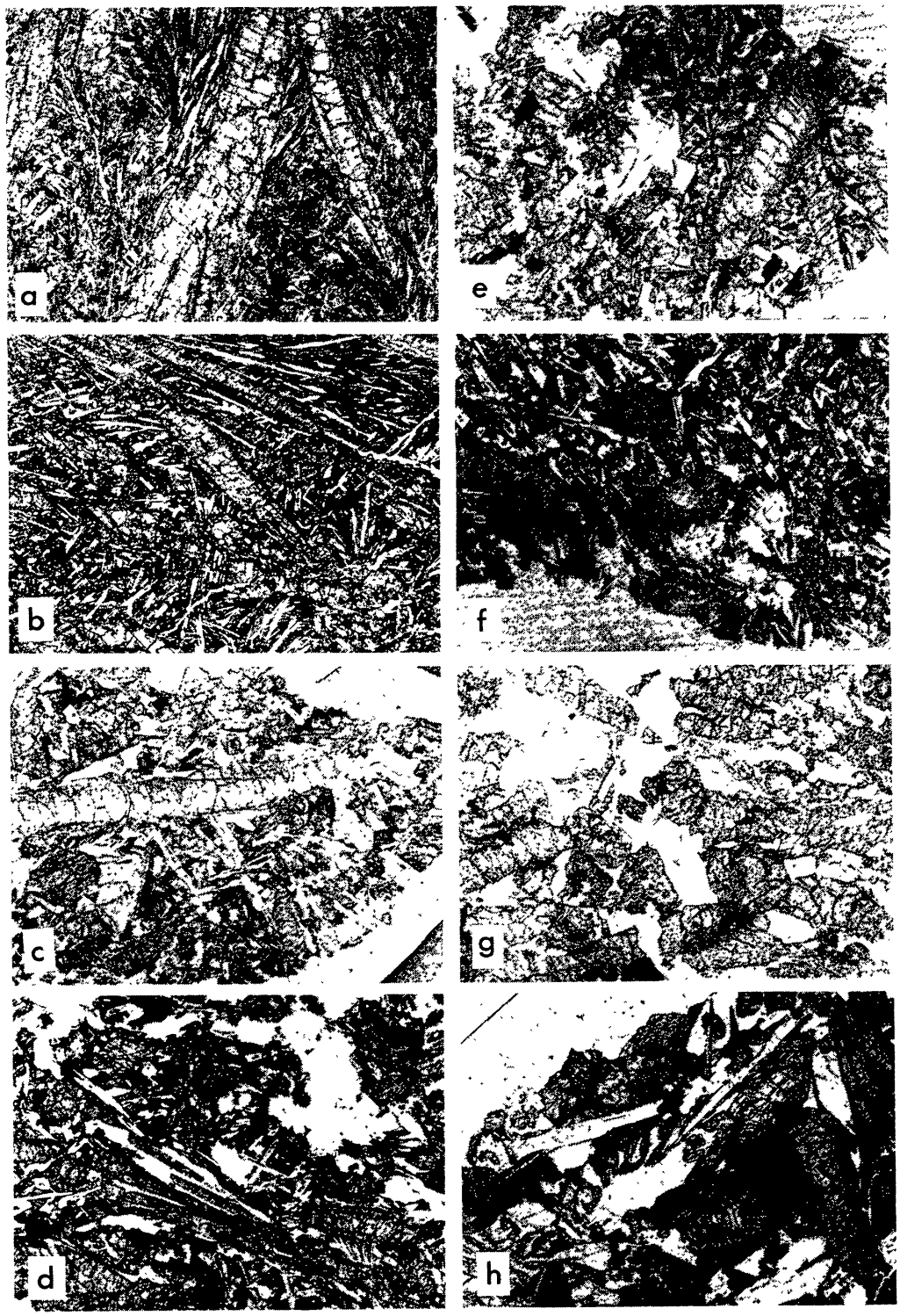

Fig. 2. Quartz-normative basalts ranked in order of decreasing cooling rate at which the phenocrysts grew (Table 1) based on comparisons with experimentally crystallized basalt. Porphyritic radiate basalts are shown in a and b, the porphyritic basalt in c is "transitional," and porphyritic subophitic basalts are shown in d–h (Table 2). Each photomicrograph is 12 mm wide: (a) 15476,32; (b) 15495,92; (c) 15475,14; (d) 15058,126; (e) 15075,40; (f) 15076,72; (g) 15065,89; and (h) 15085,19.

Table 2. On basalt textural classification.

Vitrophyric (15485, 15486, 15597)	
Phenocrysts	—elongate skeletons
Matrix	—cryptocrystalline, locally spherulitic
Porphyritic, spherulitic (15499, 15595, 15596)	
Phenocrysts	—elongate, euhedral, slightly skeletal
Matrix	—pyroxene and plagioclase in fan spherulites
Porphyritic, radiate (15476, 15495, 15475)	
Phenocrysts	—elongate, subhedral to euhedral; much larger than in vitrophyric and spherulitic samples
Matrix	—acicular radiate plagioclase and fan spherulitic pyroxene together with subequant plagioclase and pyroxene
(15475 is transitional between this group and the next)	
Porphyritic, subophitic (15058, 15075, 15076, 15065, 15085)	
Phenocrysts	—elongate to subequant, subhedral to euhedral
Matrix	—subophitic to intergranular: elongate to subequant, few plagioclase skeletons and subequant pyroxene, rare fan spherulites of pyroxene

phenocryst morphology accurate to only a factor of 2 or 3. Direct comparisons are shown in Fig. 3 (compare the phenocrysts in Fig. 3a with Fig. 1b, those in Fig. 3b with Fig. 1f, Figs. 3c and 3d, Figs. 3e and 3f). There is often a range of crystal morphologies present in a single experimentally crystallized basalt and in the natural basalts such that the dominant morphologic type must be considered. This is especially true for the matrix crystals. Figures 3g and 3h show fan spherulites of pyroxene in a 5°C/hr cooling rate run and in 15476 indicating that the matrix must have cooled at near 5°C/hr but probably less than that because there is a large number of crystals similar to the matrix crystals in the 2.5°C/hr run shown in Fig. 3b.

Taylor *et al.* (1975) have placed quantitative cooling rates on some of the QN basalts. Their values are based on the kinetics of Zr partitioning between coexisting ilmenite and ulvöspinel and thus apply to subsolidus cooling only. Their values of less than 0.5°C/hr for samples 15085, 15075, 15076, and 15065 are compatible with the values in Table 1.

The apparent cooling rates at which the phenocrysts grew are generally less than the inferred cooling rates at which the matrix minerals grew, suggesting an increase of cooling rate with a decrease in the temperature of the lava. The differences are not as dramatic, however, as would result from a classic two-stage model for development of the porphyritic texture which would have equilibrium growth of the phenocrysts at depth and development of the matrix following eruption. The differences in cooling rates between phenocrysts and matrix crystals is less than 20°C/hr, and the phenocrysts have certainly grown at cooling rates (Table 1) in excess of those that could be expected in a crustal magma chamber.

The direct comparison of the textures of the experimentally crystallized and

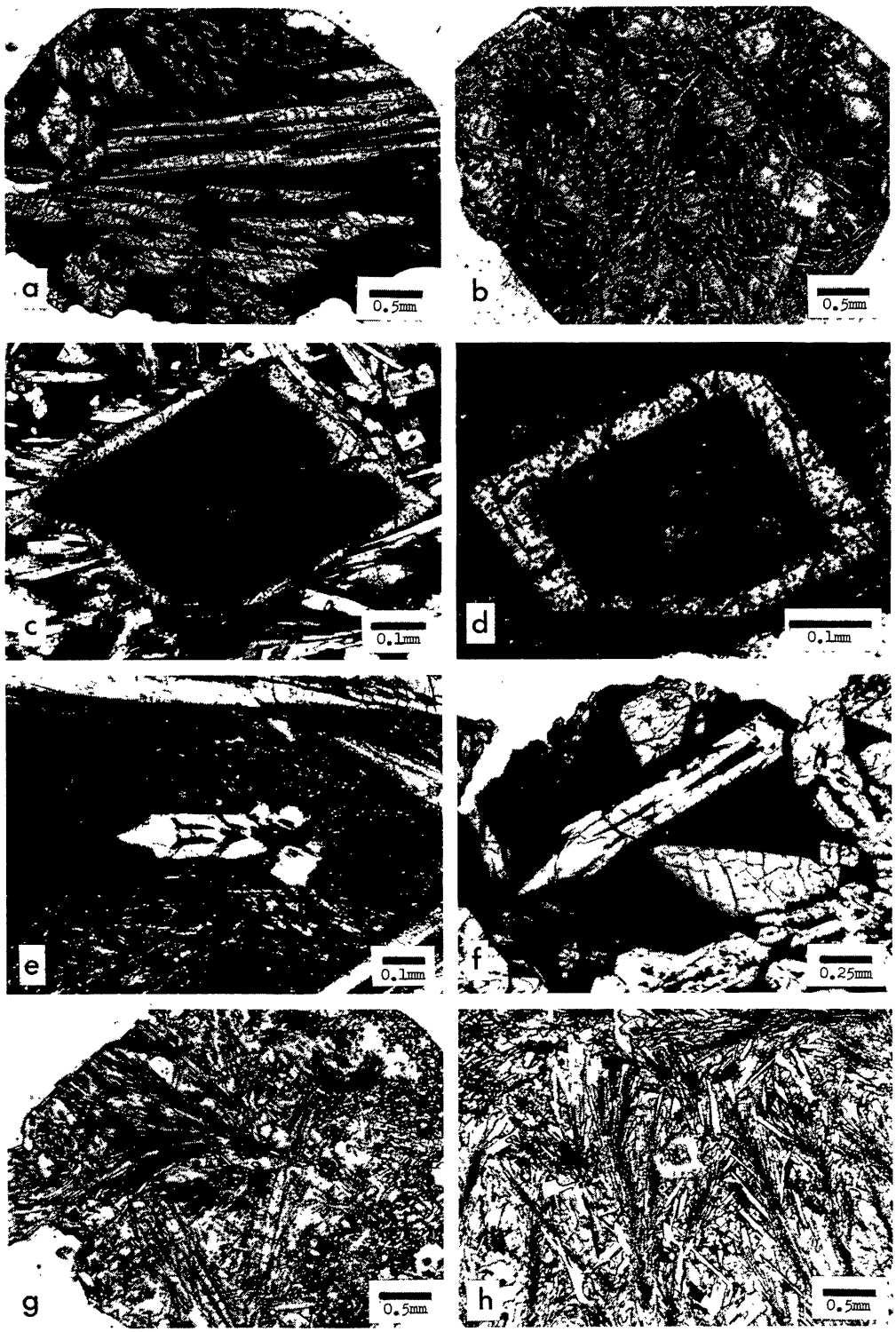

Fig. 3. Comparison of textures and crystals between experimentally crystallized basalts and natural quartz-normative basalts: (a) Cooled at 5°C/hr with very low f_{O_2}, compare Fig. 1b. (b) Cooled at 2.5°C/hr near IW buffer, compare to phenocrysts in Fig. 1f. (c) Pigeonite phenocryst grown at 2.5°C/hr, compare to phenocryst in 3d. (d) Pigeonite phenocryst in 15595,37 (see also Fig. 1e). (e) Olivine grown at 16°C/hr, compare to phenocrysts in 3f. (f) Olivine phenocrysts in 15486,22. (g) Fan spherulites of pyroxene in the matrix grown at a cooling rate of 5°C/hr, compare to 3h. (h) Fan spherulites of pyroxene in the matrix of 15476,32.

natural basalts are made for linear growth rates which approximate the cooling path through the crystallization interval in the outer portions of lava flows (Fig. 4). Toward the center of a flow the cooling rate increases with decreasing temperature (Fig. 4). The natural cooling curves may therefore, in part, account for the apparent increase in cooling rate with decreasing temperature. This interpretation, however, does not adequately explain the cooling rate changes inferred for the vitrophyres. Differences in nucleation density and changes in oxygen fugacity also affect the nature of the matrix texture and may explain the discrepancies.

Nucleation, both homogeneous and heterogeneous, is a chance event. The temperature at which the phenocryst and matrix minerals nucleate will affect their abundance and morphology. For example, if cooling is fast enough, nucleation is delayed and the crystals assume a morphology typical of growth at a larger degree of supercooling (ΔT) (Lofgren, 1974; Lofgren *et al.*, 1974). In experiments, and in the natural samples where the cooling conditions are similar, the matrix minerals need not nucleate at the same ΔT in runs cooled at the same rate. This may be caused by local abundance, or absence, of heterogeneous nuclei such that nucleation takes place readily or is delayed in one case and not the other and the morphologies of the matrix crystals will differ. Those that grow in the delayed nucleation case will resemble those typically grown at higher cooling rates. The abundance of heterogeneous nuclei is affected by the degree of superheat. The

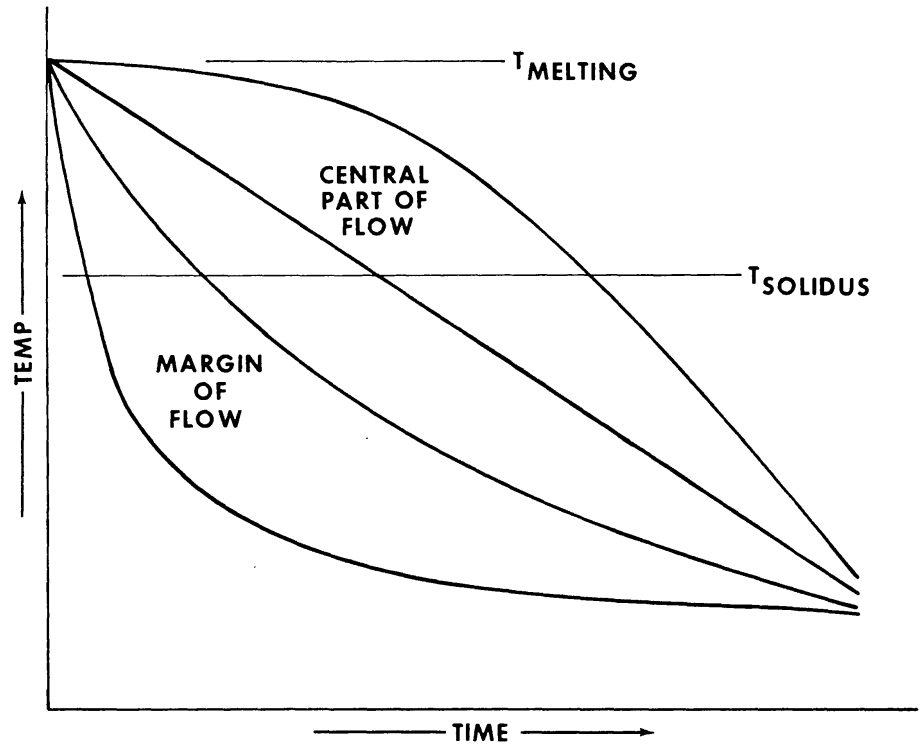

Fig. 4. Generalized time–temperature cooling curves for a basalt flow based on heat flow calculations of Jaeger (1967). The cooling curves are approximately linear through the crystallization interval near the margin of the flow and show a steady increase in cooling rate with decreasing temperature in the central part.

natural lunar lavas are anhydrous and, if brought rapidly to the surface, could be significantly superheated.

Phenomena that can affect nucleation in a natural lava that are not present in the experimental runs will also cause differences in texture between the experimental and the natural case. Turbulence in the lava while it is flowing can promote nucleation (Buckley, 1951). Settling of crystals from the more rapidly cooled outer parts of the flow where nucleation is more rapid than in the central part may initiate a change in the nucleation rate greater and at a different time than that caused by supersaturation of a second phase during linear cooling (Lofgren *et al.*, 1972). Vesicles in the QN basalts suggest the presence of a volatile phase. Lofgren and Donaldson (1975) have found that small quantities of water in the gas can increase the nucleation rate.

Variations in oxygen fugacity also have an effect on the matrix texture. In several runs the f_{O_2}, which was usually maintained at, or slightly below IW, drifted significantly lower. When this occurred the matrix was cryptocrystalline (Fig. 3a) as contrasted with a much coarser grained matrix that formed at equivalent cooling rate but higher f_{O_2}. The proportions of cryptocrystalline material to glass vary considerably. This affect of f_{O_2} is also related to nucleation because the development of the cryptocrystalline material requires a nucleation event.

The manner in which the oxygen fugacity affects the crystal size and nucleation density is not clear. One possibility is that with decreasing f_{O_2}, Fe-metal precipitates, thereby lowering the Fe content of the residual melt and raising its liquidus temperature and viscosity. The result would be to rapidly increase ΔT and inhibit nucleation and growth of crystals. Brett (1975) and Gibson *et al.* (1975) have shown that sulfur volatilization would result in f_{O_2} variation in the magma. The cryptocrystalline matrices of the vitrophyres are rarely glass, but contain large numbers of sub-micron crystals or spherulites with closely spaced sub-micron fibers. Whether these crystals form during the initial cooling of the rocks or by subsequent devitrification is difficult to determine.

Geologic Setting

The data obtained in experimental studies reported here can be combined with previous geologic and chemical studies to yield a more comprehensive understanding of the origin and history of the QN basalts. For this purpose, the geologic and chemical evidence are reviewed in the next sections.

The geology of the Apollo 15 basalts has been discussed most extensively by Swann *et al.* (1972), ALGIT (1972), Howard *et al.* (1972), and Schaber (in press). There remains, however, important geologic evidence that has not been given due consideration in either formulating studies of the QN basalts or interpreting their stratigraphy.

QN basalt samples greater than 40 g were collected at four localities (Fig. 5): Elbow Crater, Station 1; Dune Crater, Station 4; ALSEP Site, Station 8; and Hadley Rille, Station 9a. They have also been identified in rake samples from St. George Crater, Station 2 and the Rille (Dowty *et al.*, 1974). Only at the Rille and

Fig. 5. Geologic traverse map of the Apollo 15 landing site. The ALSEP site is within 200 m of the lunar module site. Taken from NASA Lunar Photomap 41B4S4(25).

Rhysling Crater, Station 3, were olivine-normative basalts greater than 40 g collected.

All four basalt samples from Elbow Crater are quartz normative. They were collected at 20–40-m intervals as a radial sample (Swann *et al.*, 1972; Fig. 5-56)* from the ejecta blanket on the east side of the crater. The locations, however, are not simply related to their distances from Elbow Crater because they have been moved by more recent cratering events (Swann *et al.*, 1972).

All six basalts collected at Dune Crater are quartz normative (15475, 15476, 15495, 15485, 15486, 15499; p. 5-79 to 5-82). Samples 15475, 15476, and 15495 were collected 30 m away from the Dune Crater rim (Fig. 5-74). The other three samples (15485, 15486, and 15499) were collected from a large filleted boulder on the rim of Dune Crater at the junction of a smaller (100 m) younger crater (Fig. 6). Sample 15499 can be accurately located on photographs of this boulder, but 15485 and 15486 are less well located. They apparently were resting on the surface of the boulder about 0.5 m away from 15499 (Fig. 6b) and are certainly part of this boulder, but may not be from the exact location on the boulder from which they were collected.

One QN basalt was collected at the ALSEP site (15058; p. 5-102). It was perched on the surface and apparently not related to a specific physiographic feature.

The Hadley Rille is the only station where abundant large samples of both olivine-normative and quartz-normative basalt were collected in close proximity, and even here there is a definite spatial relationship, with the quartz-normative samples being closest to the Rille edge (Fig. 5-115). QN basalt samples 15595 and 15596 were broken from an approximately 1-m diameter boulder (Fig. 7), that astronauts Scott and Irwin described as bedrock. The samples are approximately 20 cm apart. The boulder is one of many concentrated along the edge of the Rille (Fig. 8). It is not now bedrock, but has probably only recently been dislodged from the underlying bedrock and not moved significantly from its original position. Another QN basalt, 15597, was collected near this boulder, but was not photographed and consequently has not been accurately located.

Olivine-normative basalts 15535 and 15536 were collected from a large boulder that also qualifies as slightly displaced bedrock. This boulder is about 12 m northeast of, and slightly upslope from the 15595–596 boulder (Fig. 5-115) and thus stratigraphically higher. This boulder is isolated somewhat from the concentration of boulders that mark the Rille edge (Fig. 5-119).

Isolated outcrops representing nearly 60 vertical meters exposed in the west wall of Hadley Rille provide a unique opportunity for examining the mare basalts in cross section. Howard *et al.* (1972) have proposed the following stratigraphic section. The section is dominated by a massive unit 15–20 m thick (Fig. 9). Internal structures such as layering, horizontal parting, and different weathering patterns suggest that more than one flow exists between different massive outcrops if not within a single outcrop. Boulders up to 15 m in diameter lying on the sides and at

*Further references to figure or page numbers preceded by a five (5-) are from Swann *et al.* (1972).

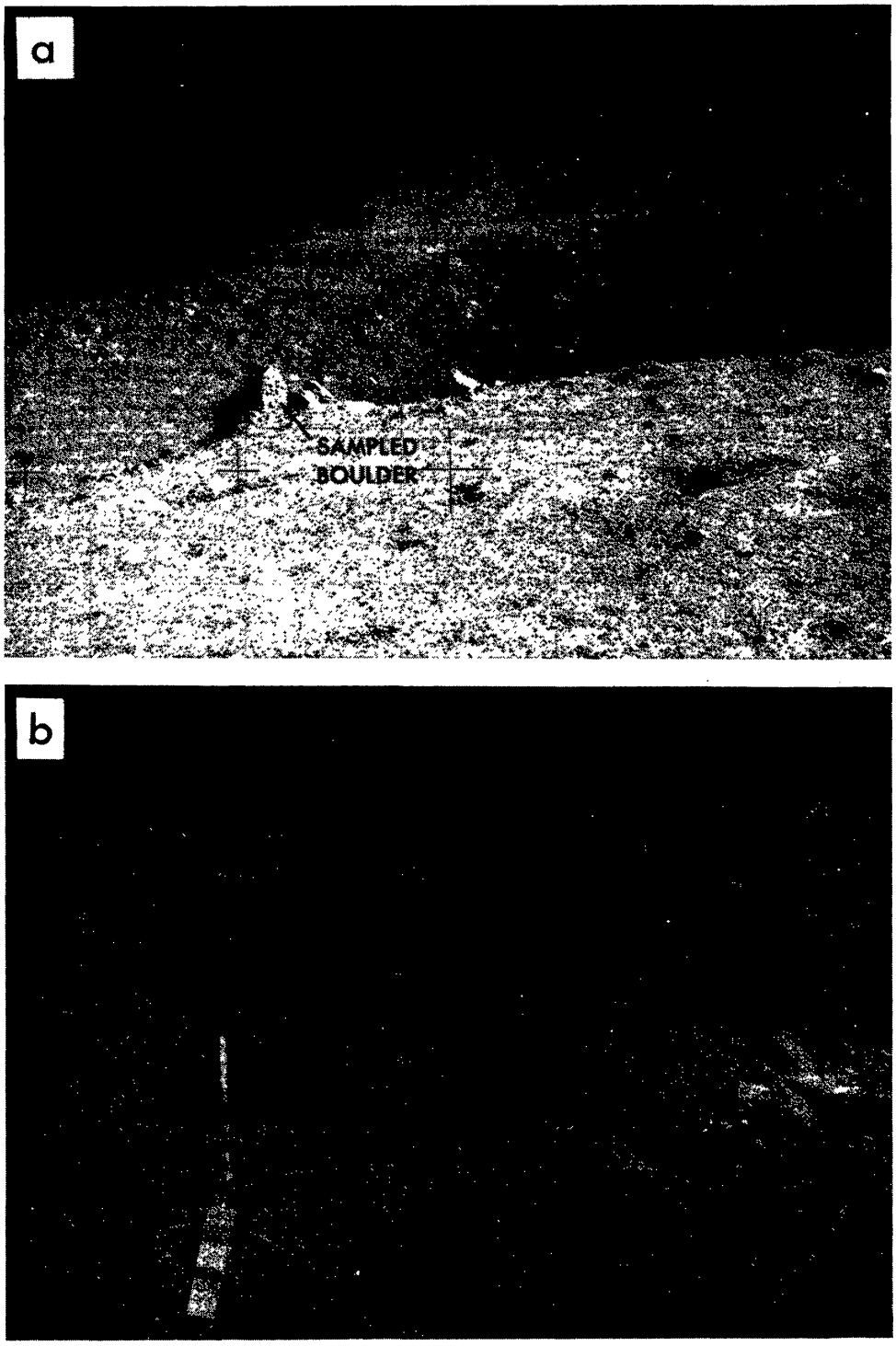

Fig. 6. Dune Crater (Station 4) sampling site. (a) Dune crater showing the large boulder on the crater rim that was sampled by Scott and Irwin. NASA Photo AS15-90-12243. (b) Close-up of sampled boulder showing the localities of 15485, 15486, and 15499. The distance between 15499 and 15485 and 15486 is approximately 42 cm. NASA Photo AS15-87-11768.

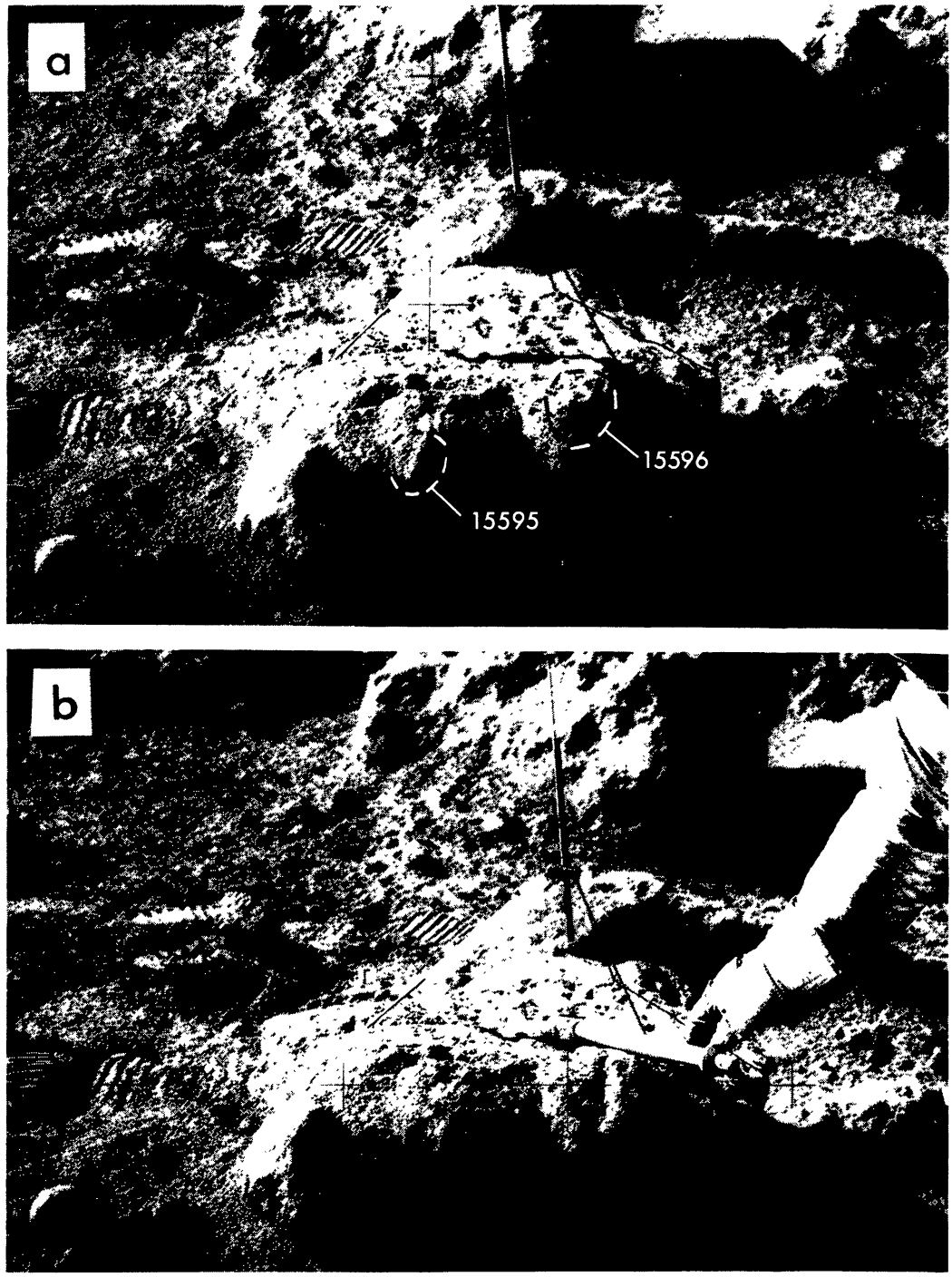

Fig. 7. Porphyritic, spherulitic basalt boulder sampled at the Rille edge (Station 9a). (a) Before sampling, NASA Photo AS15-82-11143. (b) After sampling 15595 and 15596. Samples are about 20 cm apart. NASA Photo AS15-82-11146.

the bottom of the Rille suggest the presence of at least one flow of comparable thickness. Overlying the massive unit is a darker, thinner unit (2–3-m maximum vertical exposure) that appears to be in sharp contact with the massive unit. Boulders in the regolith overlying this dark unit resemble the massive unit

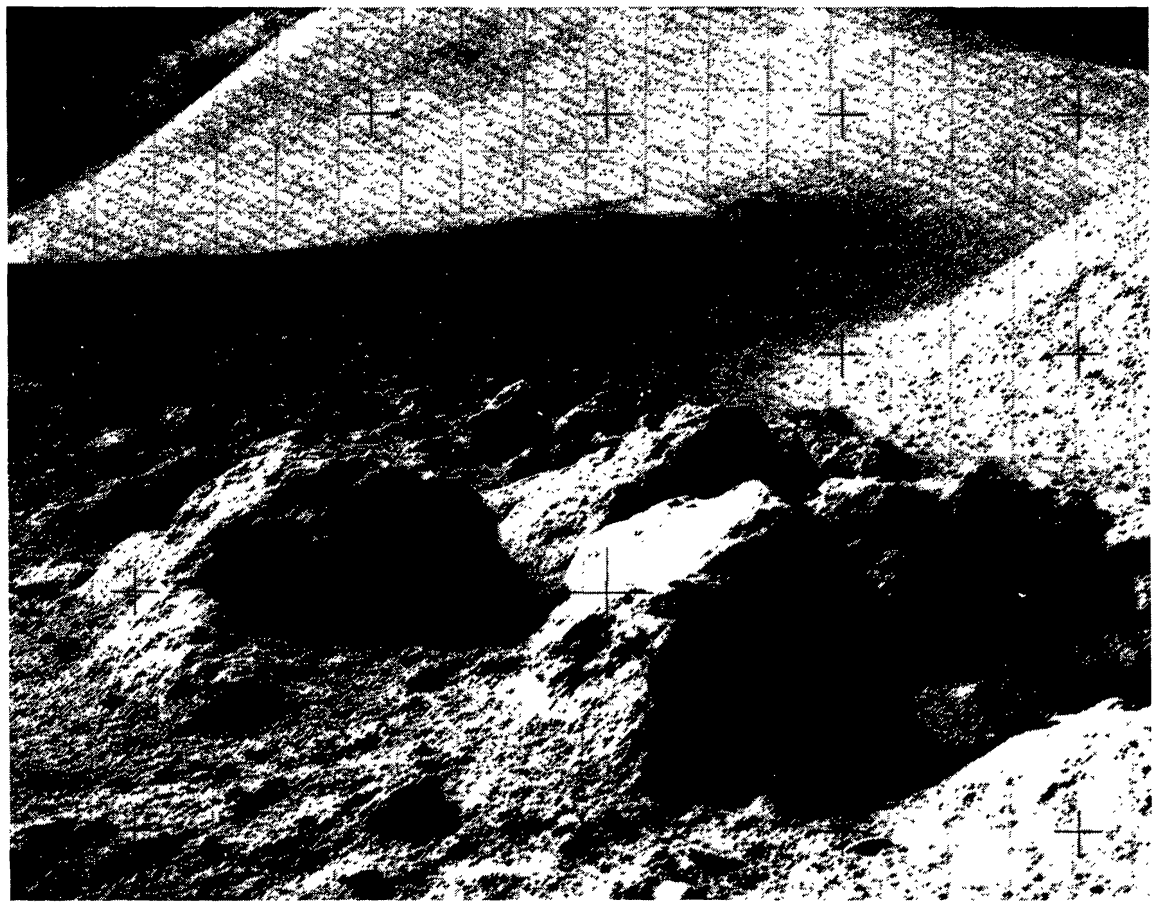

Fig. 8. East side of Hadley Rille photographed from Station 9a near the spherulitic basalt boulder looking south toward St. George Crater. The boulders have been displaced from underlying bedrock by recent impacts. NASA Photo AS15-82-11147.

suggesting the presence of yet another unit that is not seen in outcrop. There is only one exposure of the lowest observed unit. The outcrop is 8 m high and 12 layers, 1–3 m thick (Fig. 9), are tentatively identified. Single vertical fractures cut across apparent layers suggesting that they may not all represent separate lava flows.

Vesicles of widely varying dimensions are observed in the samples, large boulders, and in outcrops exposed and photographed on the far side of the Rille. The vesicles vary from less than 1 mm in hand specimen to 50 cm in outcrops exposed in the Rille walls. Most are rounded, often amoeboid and are irregularly distributed with respect to any apparent flow surface. Distinct parallel layers can also be seen in many boulders and appear to result from varying concentrations of vesicles.

CHEMISTRY AND PETROGENESIS

Of the QN basalts listed in Table 1, all have been analyzed, except 15596 which is classified as quartz normative on the basis of its petrography and because of its

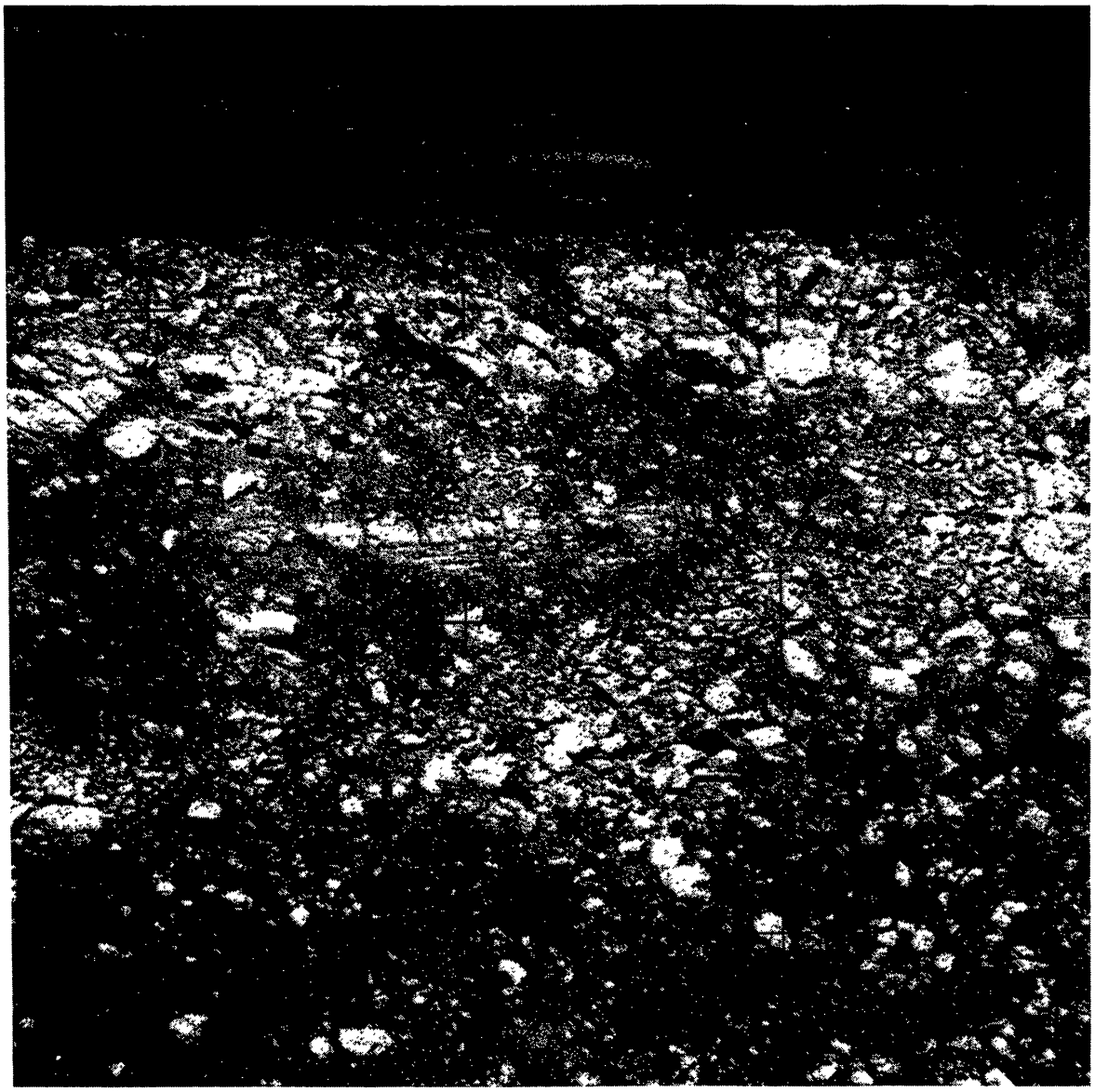

Fig. 9. West side of Hadley Rille photographed from Station 9a with a 500-mm lens. Massive basalt crops out above a more thinly layered basalt. The thinly layered lavas that overlie the massive unit are not exposed here. Lower outcrop is approximately 8 m thick. NASA Photo AS15-89-12046.

obvious relationship with 15595 (Fig. 7). The chemistry of the QN basalts (Fig. 10) is distinctive compared to other mare basalts, and the variation between samples is small (Rhodes and Hubbard, 1974; Chappell and Green, 1973). Rhodes and Hubbard (1974) and Chappell and Green (1973) have shown that small amounts of MgO variation are caused by slight, and probably local, pigeonite fractionation (7–14%). The trace elements vary much more widely and cannot be explained by this small amount of crystal fractionation. Helmke *et al.* (1973) observed variations in the rare-earth elements and suggest that variations in the Sm/Eu ratio can only be accounted for by the existence of two or three parent magmas.

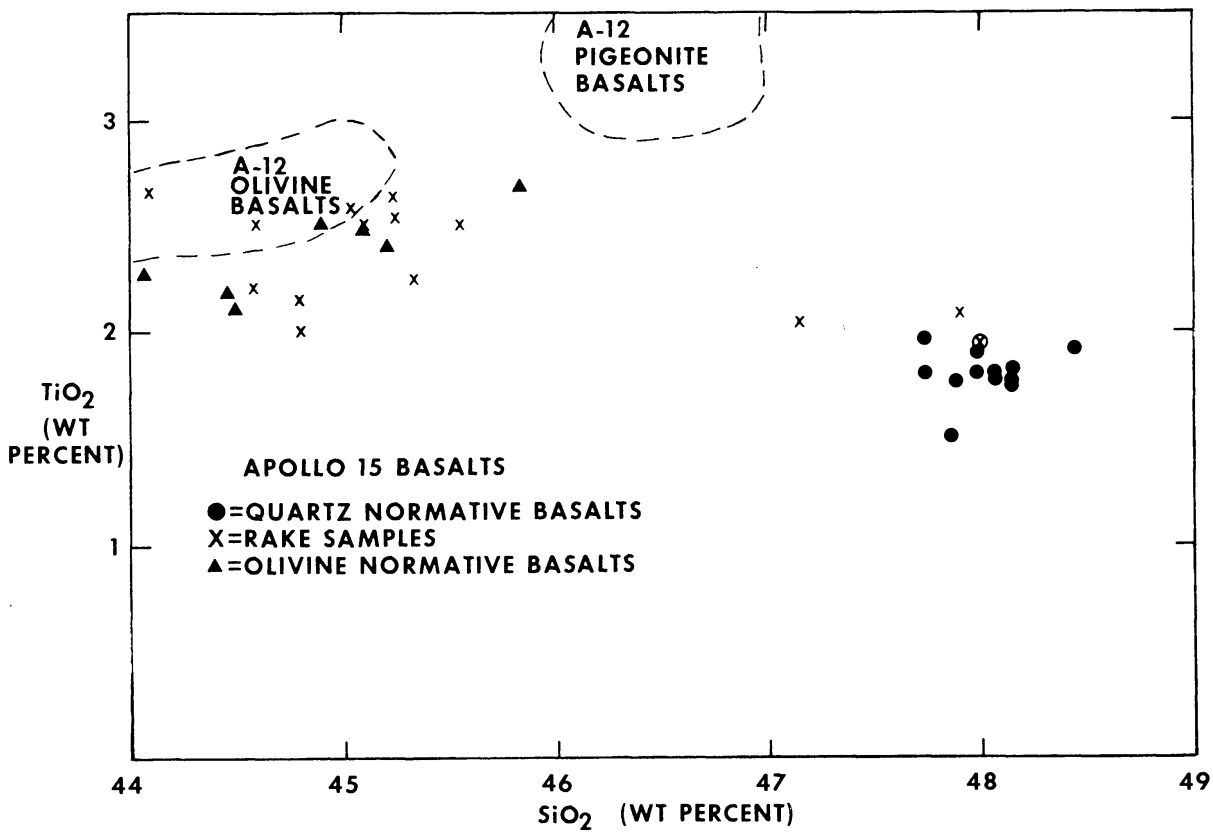

Fig. 10. Compilation of SiO_2 and TiO_2 analyses of Apollo 15 olivine- and quartz-normative basalts. All available analyses for both large rock samples and walnuts from the rake samples are plotted. The circled "×" is the average of walnuts analyzed by Dowty *et al.* (1974).

Rhodes and Hubbard (1974) point out that even though the QN basalts are the dominant basaltic rock type, the soil composition at each station is too MgO rich to be derived from QN basalt and highlands material alone. A significant amount of the olivine-normative basalt must be present. A detailed analysis of the Apollo 15 soil composition by Duncan *et al.* (1975) shows that the olivine-normative basalt is, in fact, the dominant basalt component at all stations except Spur (Station 7) and Elbow Crater and is significant at those stations.

The isotopic ages of the quartz-normative basalts are summarized by Schaber (in press) and do not show sufficiently large differences to distinguish different units. However, the olivine-normative basalts appear slightly younger.

The quartz- and olivine-normative basalts are not genetically related by low-pressure fractionation of liquidus phases (Chappell and Green, 1973; Rhodes and Hubbard, 1974; Dowty *et al.*, 1973). The high-Mg/Mg + Fe ratio and low-TiO_2 content of the QN basalts compared to the olivine-normative basalts precludes the simple removal of liquidus minerals to produce the QN basalt liquids. The low-TiO_2 contents also precludes a similar relation to mare basalts from Apollos 11, 12, and 17. Chappell and Green (1973) do, however, favor low-pressure fractionation from an olivine basalt parent and predict such a basalt would have

10% normative olivine, Mg/Mg + Fe = .53, TiO_2 = 1.5%, Al_2O_3 = 8.5%, and CaO = 9.5%. This parent magma could be produced by partial melting at 130 to 180 km.

Discussion

Significance of phenocrysts

The phenocrysts in the QN basalts have been attributed to rapid crystallization within a lava flow by Dowty *et al.* (1974), Weigand and Hollister (1973), and to more quiescent crystallization before eruption by Brown *et al.* (1972) and Humphries *et al.* (1972). Bence and Papike (1972) found no compelling evidence in favor of either case. The arguments have been reviewed most recently by Dowty *et al.* (1974). The geologic evidence, however, has been largely ignored. The documented samples collected from boulders at Dune Crater and the Hadley Rille show variations in the phenocryst morphology. There is no evidence in the photographs of these boulders that flow boundaries separate these samples. The difference in phenocryst morphology between samples 15499, 15485, and 15486 is not great (Figs. 1a,b,d), but is sufficient to show that the phenocrysts did not grow under identical conditions, but most likely at different positions in a lava flow, compatible with the distance between them (Fig. 6). There is less difference between the phenocryst morphologies in 15595 and 15596 collected approximately 20 cm apart (Fig. 7). Sample 15597 collected near this large boulder has not been documented, but most likely comes from the same lava flow. Its phenocrysts are distinctly different in both size and morphology from phenocrysts in 15595 and 15596 (compare Figs. 1c,e,f).

The experimental verification (Lofgren *et al.*, 1974) that phenocrysts of sufficient size, proper morphology, and with similar complex zoning patterns can be grown from a melt of QN basalt composition at linear cooling rates that are compatible with cooling rates in lava flows, substantiates the petrographic and crystallographic arguments of Dowty *et al.* (1974) that the phenocrysts grew on the lunar surface within the lava flow. The phenocrysts and matrix textures should then be simply attributable to position in the lava flow with anomalies caused by variations in nucleation and f_{O_2}. The large break in phenocryst size between samples 15596 and 15476 (Figs. 1 and 2) could be an artifact of selective sampling. The variation in phenocryst percentage within the vitrophyres is attributed to differences in cooling rate. Metastable growth of one phase in a melt beyond the modal amount that would be found in its more slowly cooled equivalent has been found to occur as a function of cooling rate (Lofgren *et al.*, 1974). If the Dune Crater vitrophyres represent the lower margin of the QN basalt lava flow and the Rille vitrophyres the top, crystal accumulation at the bottom of the flow may have accentuated the difference in percentage of phenocrysts.

Flow thickness

Estimates of the thickness of the QN basalt flow can be made based on three lines of evidence: the thickness of the lava flows exposed in the Rille wall

(Howard *et al.*, 1972); the depth from which samples, presumed to be from the same lava flow, were excavated and systematically collected from craters of varying sizes which consequently sample varying stratigraphic depths (Schaber, in press); and the absolute cooling rates determined for the most slowly cooled samples in the suite of samples presumed to be from one lava flow.

The photographic evidence of flow thicknesses in the Rille wall is the most direct evidence acquired during the Apollo program of the thickness of lunar lava flows and even that evidence is subject to interpretation. The maximum dimension of boulders according to Howard *et al.* (1972) sets a minimum dimension for the massive flow in the Rille wall of 15 m. The more thinly layered outcrops above and below the massive unit could be the rapidly cooled margins of one 20–30-m flow, or, more likely, could be additional thinner flows on the order of 1–3-m each. The Rille exposures then suggest flow thicknesses ranging from 1 to 30 m with a more reasonable maximum of 15–20 m.

The relationship of samples to specific craters and presumed sampling depths is much more ambiguous and probably the least definitive evidence of flow thickness. If the vitrophyric samples from the boulder at the Rille edge (15595–596) truly represent slightly displaced bedrock and the outer part of a lava flow, and if the Dune Crater vitrophyres whose presumed depth of sampling is 90–100 m (Schaber, in press) represent the bottom of the same lava flow, then the fact that the Rille outcrop is 20 m below the Dune Crater suggests a lava flow thickness of 70–80 m. This must be considered a maximum thickness because the assumption that a boulder located at a crater rim, especially a boulder as large as the Dune Crater boulder (Fig. 6), represents the stratigraphically deepest samples excavated by that crater is contradicted by detailed study of ejecta from the Ries Crater, Germany (Stöffler *et al.*, 1974). They showed that most large boulders at or near the crater rim represent near-surface bedrock and not necessarily the deepest bedrock excavated by the cratering event.

The slowest cooling rates determined for the QN basalts of less than 1.0°C/hr through the crystallization interval and between 0.5 and 0.2°C/hr for the initial subsolidus interval of 100–200°C permits calculation of a minimum flow thickness. Provost and Bottinga (1972) have provided data for the Apollo 11, high-titanium basalts that are compatible with a 2–3 m flow thickness for similar cooling rates. The only difference between the QN basalts and the high-titanium basalts that would affect the calculation of flow thickness is the viscosity, which is about two times larger and which would not change the estimated flow thickness significantly. This is a minimum thickness because the slowest cooling rate has not been determined.

If the 2–3-m flow thickness is accurate, the QN basalts may correlate with the flows overlying the massive flow unit exposed in the Rille wall. This correlation must be made carefully because the east rim of the Rille is 30–40 m above the west rim (Howard *et al.*, 1972) and correlation of lava flows across the Rille may not be valid.

Number of flows

The number of QN basalt flows, and consequently the maximum possible number of parent magmas are important considerations in understanding the petrogenesis of the basalts. The petrographic and experimental evidence are compatible with either a single flow or several flows of similar composition and cooling histories. The geologic evidence is equally ambiguous. Samples with a particular textural character are associated with a particular sample locality. Only at Dune Crater were coarse-grained and vitrophyric QN basalts collected at the same station, and even here they were collected 30 m apart. The Elbow Crater and ALSEP site samples were all coarse-grained and could be from a different flow, but just as easily could be from different parts of the same flow sampled from different depths by cratering.

The chemical evidence is equally ambiguous. The consistent major-element chemistry is compatible with the petrographic, geologic, and experimental evidence that the lavas came to the surface totally liquid and that there was very little if any crystal fractionation prior to eruption. The conflicting trace-element data is not easily explained. Helmke *et al.* (1973) maintain that unrepresentative samples cannot explain the difference between the vitrophyres. Dowty *et al.* (1974) point out, however, that the differences are very small, about 1 ppm, and that sampling errors may still be a problem (Mason *et al.*, 1972; Nava, 1974). It may also be presumptious to assume that equilibrium partitioning of trace elements is not affected by nonequilibrium crystallization in these rapidly cooled rocks.

The trace-element data is available for only a limited number of rocks. A good test of the validity of trace-element variations would be to analyze samples from the same boulder which are obviously from the same parent magma. Two such tests are possible with the QN basalts: compare 15595 with 15596; and 15499 with 15485 and 15486. These boulder samples should be analyzed before any final conclusions based on trace elements are made on the number of flows and parent magmas. Thus, until more conclusive evidence is presented, the QN basalt samples should be considered textural variants of a single lava flow and consequently a single parent magma.

Relations to olivine-normative basalt

The stratigraphic and petrogenetic relations between the olivine-normative and QN basalt are reasonably clear. The outcrop relations of the 15535–536 boulder to the 15595–596 boulder, the soil composition, and the apparently younger isotopic ages, place the olivine-normative basalt stratigraphically above the QN basalt. The sparcity of large olivine basalt samples away from the Rille may indicate either that it is not widespread or that it has been largely pulverized and incorporated into the soil. The large proportion of olivine-normative basalt shown to be in the soil by Duncan *et al.* (1975) favors the latter explanation. The reason for presence of large samples only at the Rille edge has been explained by Swann *et al.* (1972) as the winnowing effect of cratering at the Rille edge. Thus the

QN basalt samples have been exposed by craters that ejected bedrock, whereas large samples of olivine-normative basalt are probably buried within the 5m of regolith that blanket the Apollo 15 site, except at the Rille edge. The dominance of olivine basalt in rake samples appears consistent with this suggestion.

The compositional differences between the two basalt types preclude any common fractionation or partial melting history. Their close spatial and age relationships suggest an effective mechanism for cleanly tapping magma sources to significant depths in the crust.

SUMMARY

The QN basalts are most likely samples of at least a 2–3-meter flow that was erupted onto the lunar surface essentially free of crystals. It is probably the low-pressure fractionation product of an olivine basalt. This olivine basalt is not related to olivine-normative basalts that overlie the QN basalts at the Apollo 15 site and would have a higher Mg/Mg + Fe value and a lower TiO_2 value. The olivine basalt was probably derived from 130–180 km by partial melting.

Acknowledgments—We greatly appreciate the assistance of J. W. Minear in the calculation of cooling curves for lavas. Discussions with R. J. Williams and J. M. Rhodes were particularly fruitful. C. H. Donaldson thanks The Lunar Science Institute for a Visiting Graduate Fellowship and the Natural Environment Research Council (U.K.) for financial support. T. M. Usselman is supported by an NRC–NASA resident research associateship. The Lunar Science Institute is operated by the Universities Space Research Association under contract No. NSR 09-051-001 with the National Aeronautics and Space Administration. This paper is The Lunar Science Institution Contribution No. 219.

REFERENCES

ALGIT (Apollo Lunar Geology Investigation Team) (1972) Geological setting of the Apollo 15 samples. *Science* **175**, 407–415.

Bence A. E. and Papike J. J. (1972) Pyroxenes as recorders of lunar basalt petrogenesis: Chemical trends due to crystal–liquid interaction. *Proc. Lunar Sci. Conf. 3rd*, p. 431–469.

Brett R. (1975) Reduction of mare basalts by sulfur loss (abstract). In *Lunar Science VI*, p. 89–91. The Lunar Science Institute, Houston.

Brown G. E. and Wechsler B. A. (1973) Crystallography of pigeonites from basaltic vitrophyre 15597. *Proc. Lunar Sci. Conf. 4th*, p. 887–900.

Brown G. M., Emeleus C. H., Holland J. G., Peckett A., and Phillips R. (1972) Petrology, mineralogy and classification of Apollo 15 mare basalts. In *The Apollo 15 Lunar Samples* (editors J. Chamberlain and C. Watkins), p. 40–44. The Lunar Science Institute, Houston.

Buckley H. E. (1951) *Crystal Growth*. Wiley, New York.

Chappell B. W. and Green D. H. (1973) Chemical composition and petrogenetic relationships in Apollo 15 mare basalts. *Earth Planet. Sci. Lett.* **18**, 237–246.

Dowty E., Prinz M., and Keil K. (1973) Composition, mineralogy, and petrology of 28 mare basalts from Apollo 15 rake samples. *Proc. Lunar Sci. Conf. 4th*, p. 423–444.

Dowty E., Keil K., and Prinz M. (1974) Lunar pyroxene-phyric basalts: Crystallization under supercooled conditions. *J. Petrol.* **15**, 419–453.

Duncan A. R., Sher M. K., Abraham Y. C., Erlank A. J., Willis J. P., and Ahrens L. H. (1975) Compositional variability of the Apollo 15 regolith (abstract). In *Lunar Science VI*, p. 220–222. The Lunar Science Institute, Houston.

Gibson E. K., Chang S., Lennon K., Moore G. W., and Pearce G. W. (1975) Sulfur abundances and distributions in mare basalts and their source magmas. *Proc. Lunar Sci. Conf. 6th.* Vol. 2.

Helmke P. A., Blanchard D. P., Haskin L. A., Telander K. M., Weiss C. K., and Jacobs J. W. (1973) Major and trace elements in igneous rocks from Apollo 15. *The Moon* **8**, 129–148.

Howard K. A., Head J. W., and Swann G. A. (1972) Geology of Hadley Rille. *Proc. Lunar Sci. Conf. 3rd,* p. 1–14.

Humphries D. J., Biggar G. M., and O'Hara M. J. (1972) Phase equilibria and origin of Apollo 15 basalts etc. In *The Apollo 15 Lunar Samples* (editors J. Chamberlain and C. Watkins), p. 103–107. The Lunar Science Institute, Houston.

Jaeger J. C. (1967) Cooling and solidification of igneous rocks. In *Basalts*: *The Poldervaart Treatise on rocks of Basaltic Composition* (editors H. H. Hess and A. Poldervaart), Vol. 2, p. 503–536. Wiley-Interscience, New York.

Lofgren G. E. (1974) An experimental study of plagioclase crystal morphology: Isothermal crystallization. *Amer. J. Sci.* **274**, 243–273.

Lofgren G. E. and Donaldson C. H. (1975) Phase relations and non-equilibrium crystallization of ocean ridge tholeiite from the Nazca plate (abstract). *EOS* (*Trans. Amer. Geophys. Union*) **56**, 468.

Lofgren G. E., Donaldson C. H., Williams R. J., Mullins O., Jr., and Usselman T. M. (1974) Experimentally reproduced textures and mineral chemistry of Apollo 15 quartz normative basalts. *Proc. Lunar Sci. Conf. 5th*, p. 549–567.

LSPET (1972) The Apollo 15 lunar samples: A preliminary description. *Science* **175**, 363–375.

Mason B., Jarosewich E., Melson W. G., and Thompson G. (1972) Mineralogy, petrology, and chemical composition of lunar samples 15085, 15256, 15271, 15471, 15475, 15476, 15535, and 15556. *Proc. Lunar Sci. Conf. 3rd*, p. 785–796.

Nava D. F. (1974) Chemical compositions of some soils and rock types from the Apollo 15, 16, and 17 lunar sites. *Proc. Lunar Sci. Conf. 5th*, p. 1087–1096.

Papike J. J., Bence A. E., and Ward M. A. (1972) Subsolidus relations of pyroxenes from Apollo 15 basalts. (editors J. Chamberlain and C. Watkins), In *The Apollo 15 Lunar Samples*, p. 144–148. The Lunar Science Institute, Houston.

Provost A. and Bottinga Y. (1972) Rates of solidification of Apollo 11 basalt and Hawaiian Tholeiite. *Earth Planet. Sci. Lett.* **15**, 325–337.

Rhodes J. M. and Hubbard N. J. (1973) Chemistry, classification, and petrogenesis of Apollo 15 mare basalts. *Proc. Lunar Sci. Conf. 4th*, p. 1127–1148.

Schaber G. (1975) Suggested mare stratigraphy and sample relocation. U.S. Geol. Survey Prof. Paper. In press.

Stöffler D., Dence M. R., Graup G., and Abadian M. (1974) Interpretation of ejecta formations at the Apollo 14 and 16 sites by a comparative analysis of experimental, terrestrial, and lunar craters. *Proc. Lunar Sci. Conf. 5th*, p. 137–150.

Swann G. A., Bailey N. G., Batson R. M., Freeman V. L., Hait M. H., Head J. W., Holt H. E., Howard K. A., Irwin J. B., Larson K. B., Muehlerger W. R., Reed V. S., Rennilson J. J., Schaber G. G., Scott D. R., Silver L. T., Sutton R. L., Ulrich G. E., Wilshire H. G., and Wolfe E. W. (1972) Preliminary geologic investigation of the Apollo 15 landing site. In *Apollo 15 Preliminary Sci. Report*, NASA publication SP-289, p. 5-1 to 5-112.

Takeda H., Miyamoto M., and Ishii T. (1975) Relative cooling rates of mare basalts at the Apollo 12 and 15 sites as deduced from crystallographic and chemical studies of the pyroxenes (abstract). In *Lunar Science VI*, p. 792–794. The Lunar Science Institute, Houston.

Taylor L. A., Uhlmann D. R., Hopper R. W., and Misra K. C. (1975) Absolute cooling rates of lunar rocks: Theory and application, *Proc. Lunar Sci. Conf. 6th.* This volume.

Weigand P. W. and Hollister L. S. (1973) Basaltic vitrophyre 15597: An undifferentiated melt sample. *Earth Planet. Sci. Lett.* **19**, 61–74.